The Development of a Quantitative Assay for the Detection of Grapevine Red Blotch-associated Virus in *Vitis vinifera* Identifies Significant Differences in Virus Distribution

Honors Thesis

Presented to the College of Agriculture and Life Sciences,

Cornell University

in Partial Fulfillment of the Requirements for the
Biological Sciences Honors Program

by

Felicia Jesslyn Setiono

May 2016

Drs. Jeremy R. Thompson & Keith L. Perry

Abstract

Grapevine red blotch-associated virus (GRBaV) is associated with red blotch disease which undermines optimal growth and development of grapevine (*Vitis vinifera*). Despite GRBaV's significant economical and biological impacts, existing diagnostic methods lack sensitivity and consistency. This study has developed, optimized and employed a reliable quantitative Real-Time PCR (qPCR) assay for the detection of GRBaV in a variety of host tissue types. Primers specific to GRBaV and internal host control (NADP-dependent Glyceraldehyde 3-phosphate dehydrogenase (GAPDH)) were selected for use in qPCR based on their performance in initial validation tests. Controls consisted of 1) the internal GAPDH which served as relative reference of total input DNA and as a marker for template quality, 2) a dilution series of cloned target viral DNA, and 3) negative controls of water and total nucleic acid from uninfected vines. This method was then used to quantify the amount of GRBaV in multiple infected greenhouse- (GG) and field- (FG) grown vines. Absolute and relative quantification methods were shown to be strongly correlated ($R^2 > 0.84$) for both GG and FG. Viral DNA quantities varied in different tissue types and from one plant to another between and within a location, but most significantly between GG and FG, where only 56.0% of the total samples from the latter were determined as positive compared to 98.4% for the former. Petioles were consistently found to contain higher amounts of GRBaV compared to their corresponding leaves ($P<0.05$). Leaves proximal to the main stem were found to contain higher amounts of GRBaV compared to leaves located in the apical part of the cane ($P<0.01$). Based on these findings, it is recommended that total nucleic acid extracted from multiple petioles of fully developed leaves are used for robust and reliable GRBaV diagnosis using qPCR. The described qPCR assay and recommended sampling procedures will contribute to efforts in GRBaV containment and red blotch disease control.

Introduction

Grapevine red blotch-associated virus (GRBaV) is a recently identified pathogen affecting grapevine (*Vitis* sp.) It is associated with red blotch disease which causes foliar discoloration and a significant reduction in berry sugar content (Al Rwahnih et al. 2013). GRBaV was first identified by two groups independently – one in California and the other at Cornell University - using next-generation sequencing and a rolling circle amplification method (Al Rwahnih et al. 2013; Krenz et al. 2012). Its sequence, though revealing a genome organization that resembled that of monopartite viruses from the family *Geminiviridae*, appeared to represent a separate lineage from a novel putative genus.

Geminiviruses are considered globally to be one of the most important emerging plant pathogens. Especially in tropical and sub-tropical regions of the world, geminiviruses are known to be substantial barriers to agricultural productivity. As geminiviruses spread towards more temperate regions due to climate change and a concurrent migration of their insect vectors, the viruses are becoming a significant threat to crops grown in North America (Mansoor et al. 2003; Mansoor et al. 2006). Additionally, new viruses and diseases may emerge in previously unaffected crops due to the viruses' ability to exchange genetic material between related viruses (within *Geminiviridae*) and their satellites.

GRBaV has been detected in vines from eight states (California, Florida, Maryland, New Jersey, New York, Oregon, Pennsylvania, and Virginia) within the United States, two provinces in Canada (British Columbia and Ontario (Sudarshana et al. 2015) and possibly outside of North America; however, the true extent of the spread of the virus globally is unknown, partly due to difficulties in diagnosing infection. Moreover, the mode of transmission of GRBaV is still not completely known. Clades and isolates within a clade of GRBaV were not correlated with spatial

proximities of infected vines planted within a field. Many GRBaV-infected cultivars from one country also had virus isolates belonging to different clades (Rwahnih et al. 2015).

Red blotch disease shares many symptoms attributed to grapevine leafroll disease which is caused by several species of *Grapevine leafroll-associated virus* (GLRaV); such as reddening of leaves (in red varieties) and leaf curling, thereby making any visual diagnosis difficult. Moreover, depending on the season, symptoms of red blotch may fail to show at all. The virus is known to affect several grapevine varieties such as Cabernet Franc, Cabernet Sauvignon, Merlot, Petite Sirah, Petit Verdot and Zinfandel (National Clean Plant Network [NCPN] 2013). The disease has a large economic impact impeding grape production in the United States (Naidu et al. 2014). Grapes are used not only for the production of fresh fruits, but also for wines, juices, raisins, jellies, vinegars, and oils. The United States is one of the top grape producing countries, smaller only in comparison to People's Republic of China and Italy. The grape, wine, and juice industries are continually growing in nearly every state, yielding more than $162 billion annually in revenue (Naidu et al. 2014). In 2013, total grape production in the United States was 8 million tons, resulting in an 8.8% increase in value for the industry from the previous year (USDA, 2014). Vine health is affected by red blotch disease through a reduction of photosynthesis and stomatal conductance, berry weight and anthocyanin level at harvest, and pruning weight. Fruit yield and quality are reduced; a 2.65 and 1.0° Brix reduction has been found in fruit juice of Cabernet Sauvignon and Chardonnay grapevines, respectively (Sudarshana et al. 2015).

Continuously increasing production and demand for grapes and grape-derived products concomitantly stimulate increasing efforts to eradicate grapevine-affecting pathogens and diseases. Grapevines are targets for many different pests and pathogens. More than 60 different viruses from 30 different genera are found to affect grapevines (Naidu et al. 2014). Grapevines

are vegetatively propagated, so the use of contaminated rootstock materials for propagation allows for the easy introduction of viruses into new vineyards, but makes eradication of such viruses extremely difficult. Transmission of grapevine viruses can also be done through insect vectors. However, some viruses still have unknown vectors such as GLRaV-2 and -7, as well as GRBaV (Naidu et al. 2014). Disease control strategies to limit virus spread and dissemination require diagnostic methods which are specific, sensitive, and can be done rapidly (Herrera-Vasquez et al. 2015). Several methods have been utilized in the discovery and detection of grapevine viruses; initially conventional methods such as virion purification and cDNA cloning were used. These conventional methods were soon replaced by serological and nucleic-acid base or molecular techniques such as ELISA, immunoabsorbent electron microscopy (ISEM), polymerase chain reaction (PCR), micro- and macroarrays, and reverse transcription polymerase chain reaction (RT-PCR) (Rwahnih et al. 2015; Hull 2014). Serological and molecular techniques are advantageous in that they quickly and sensitively allow the measurement of viral gene expression in the presence of other background genetic material such as that of host material. These latter methods however, still pose limitations in the detection of most grapevine viruses. Using standard molecular biological techniques such as PCR to accurately detect viruses in grapevine is often difficult, due to high levels of polysaccharides and polyphenolic compounds found in tissues (Reid et al. 2006), and also due to the commonly low titer of the virus in this host; GRBaV is believed, like most grapevine viruses, to be limited to the phloem. Virus quantification in the past has also been done using electrophoresis and Northern blot hybridization. However, these methods were often time consuming, laborious, insensitive, and highly variable (Feng et al. 2006; Hull 2014).

Quantitative real-time polymerase chain reaction (qPCR) assay, a highly sensitive molecular method was developed and was first commercialized in 1996. It has since been

increasingly used in basic research, pathogen detection, and biomedical diagnostics (Pabinger et al. 2014). qPCR is able to simultaneously detect changes in the concentration of nucleic acid as it is being amplified thereby allowing a more accurate measurement of how much target nucleic acid was in the reaction in the first place. Due to reaction saturation, visual assessment of the amount of final PCR product in a conventional PCR makes inferences on the initial template concentration impossible. After all, the final amount of amplicon generated and available to be assessed is confounded by many factors present in a PCR reaction such as inhibitors and by-products (Mackay et al. 2002). In comparison to other commonly used diagnostic methods such as ELISA and conventional PCR, qPCR is more sensitive, specific, and rapid (Hull 2014). Moreover, qPCR methodology is also associated with the reduced risk of carry-over contamination due to the elimination of multiple PCR product handling steps and post-PCR detection procedures (Mackay et al. 2002). qPCR plays an increasingly important role used in quantification and genotyping experiments, gene expression studies, advances in clinical research and routine diagnostics in the field of microbiology, veterinary science, pharmacology, biotechnology, toxicology, and agriculture (Navarro et al. 2015). The ability to accurately quantify viral load allows researchers to measure levels of infection, study virus-host interactions and responses of antiviral therapy in clinical settings such as viral reactivation and persistence behavior of viruses (Mackay et al. 2002). Since it is highly sensitive and reproducible, qPCR has been considered to be one of the most reliable methods available to quantify and detect gene expression (Feng et al. 2006; Mirmajlessi et al. 2015). It has been used in detecting pathogens of bacterial, fungal and viral origins and to assess the expression levels of many forms of genetic materials including messenger-, micro-, small inhibiting- and small nuclear RNA (Pabinger et al. 2014; Navarro et al. 2015).

The objectives of this study are to design a consistent and reproducible quantitative assay for GRBaV detection in grapevine, to determine the amount of GRBaV in different infected host plant tissues, and overall, to establish an optimized sampling method to detect and diagnose red blotch disease. Generally qPCR uses one of two different approaches to quantify the target molecule; absolute and relative. The former gives a definitive number of target DNA molecules present using an external standard or calibration curve from a template with known concentration while the latter gives the amount of the target molecule in different samples relative to a reference gene (Yuan et al. 2006). Several mathematical models have been developed to present data from qPCR analyses; the comparative C_T method is the most commonly used for relative quantification studies. Protocols and guidelines for ensuring reliable qPCR methodology have been developed and summarized in the Minimum Information for Publication of Quantitative Real-Time PCR Experiments (MIQE) guidelines (Bustin et al. 2009). In the experiments described below, both relative and absolute quantification approaches were developed and optimized using standard established methodology to ensure a robust, reliable and sensitive GRBaV diagnostic method for both greenhouse and field grown vines.

Information regarding these experiments will aid our understanding of the spatial (and temporal) variation in virus titer within the host plant and set the groundwork for studies into the biology of GRBaV. Since it is still not known how the virus is spread in field conditions, it is imperative to develop a method to accurately identify and detect the virus. An optimized detection assay combined with an optimal sampling strategy will allow for easier detection of the virus in the future and thus improve our ability to prevent introduction and spread of the virus in new vineyards.

Methods and Materials

1. Total nucleic acid extraction

The extraction of total nucleic acid (TNA) from grapevine tissue was modified from the CTAB-based protocol described by Gambino et al. (2008). 100mg of plant tissue was ground in liquid nitrogen (N_2) using a mortar and pestle. 500µl extraction buffer (2% CTAB, 2.5% PVP-40, 2 M NaCl, 100 mM Tris-HCl pH 8.0, and 24 mM EDTA pH 8.0) pre-heated to 65ºC was added to the mortar. The resulting homogenate was transferred to a microcentrifuge tube and 10µl β-mercaptoethanol was immediately added. The tube was incubated with mixing (at 750rpm) at 60°C for 1 hour. An equal volume of chloroform: isoamyl alcohol (24:1 v/v) was added before vortexing vigorously until an emulsion formed. The tube was centrifuged at 11,000 x g for 10 min at 4°C. The supernatant was transferred to a clean microcentrifuge tube and 0.7 volume of ice-cold isopropanol added and mixed before centrifuging at full speed (13,000 x g) for 15 min at 4°C. The liquid was discarded and the resulting pellet was washed with 500 µl 70% ethanol by centrifuging for another 2 min. The tube was then inverted to air dry and the pellet re-suspended in 50 µl RNase-free water. The quantity and quality of TNA extracted was estimated both spectrophotometrically (GE NanoVue Plus Spectrophotometer) and visually by separating the extracted TNA on a 1% agarose gel in 0.5x tris-acetate (TAE) buffer (Sambrook and Russell 2001). For a qPCR assay, the concentration of all TNA samples was normalized to 50ng/µl. All TNA samples, original and normalized, were stored at -20°C.

2. Primer design and selection

Optimal virus-specific and housekeeping (internal control) primers were designed using Integrated DNA Technologies (IDT) PrimerQuest (http://sg.idtdna.com/Primerquest/Home/Index)

with default settings; these included optimal parameters of T_m 62°C, G+C content 50%, primer size 22 nt, amplicon size 100 nt. Virus-specific primer sequences were initially based on the sequence of GRBaV isolate 'JRT[456]17NOV10' (NY358) (GenBank accession JQ901105) and later adapted when necessary using alignments with all known GRBaV sequences (Figure. 1).

All primer pairs (Table. 1) were initially screened by conventional PCR with cycling conditions of 5 min 95°C (x1) and 30s 95°C, 30s 60°C (x40) using plant TNA from GRBaV-infected plants as templates. PCR products were separated on a 1% agarose gel (0.5x TAE) for gel electrophoresis. Only those primers giving unique PCR products of the expected size without any non-specific amplification (e.g. primer-dimers) were used in the subsequent validation experiments.

Table 1. Table listing primers designed and tested.

Primer	Primer abbreviation	Sequence	Name	nt	Amplicon size (bp)	Targeted gene of sequence	Accession number of targeted sequence	Nucleotide reference location
p1181	p1v	GTACCGWRYTCGACGGTATCYC	qREP1s	22	105	GRBaV C1 (Rep)	JQ901105.2	2710-2731
p1182	p2v	CACCATATCGTCTCAYTCCTAYC	qREP1as	23				2814-2792
P1183	p3v	ACATCTCTGGGYTTKGTGATATT	qREP2s	23	113	GRBaV C1		2764-2786
p1184	p4v	CTACACGCCTTGCTCATCTT	qREP2as	20				2876-2857
p1185	p5i	CACCATGAGTCTTTGGTAGAGG	qEF1s	22	119	Elongation factor 1-α	NC_012014	13422791-13422812
p1186	p6i	GCAGGATCATCTTTGGAGTTAGA	qEF1as	23				13422909-13422887
p1187	p7i	GGTGTTGGTGTCTCCATAGTT	qNADs	21	110	NADP-dependent Glyceraldehyde 3-phosphate dehydrogenase	NC_012010	5401243-5401263
p1188	p8i	CCTAGTTGCCTTGAGGTCTTT	qNADas	21				5401352-5401332
p1189	p9i	GTAGAAGGTGTGATGCCAGATT	qActina	22	102	Actin	NC_012014	20251517-20251538
p1190	p10i	GGCACAATCCAAGAGAGGTATT	qActinas	22				20251619-20251598

Primer abbreviations will be used subsequently in the paper where each number indicates a distinct primer sequence and 'v' or 'i' identifies the primer as virus specific or internal control specific, respectively.

Figure 1. (a) legend is located on page 10.

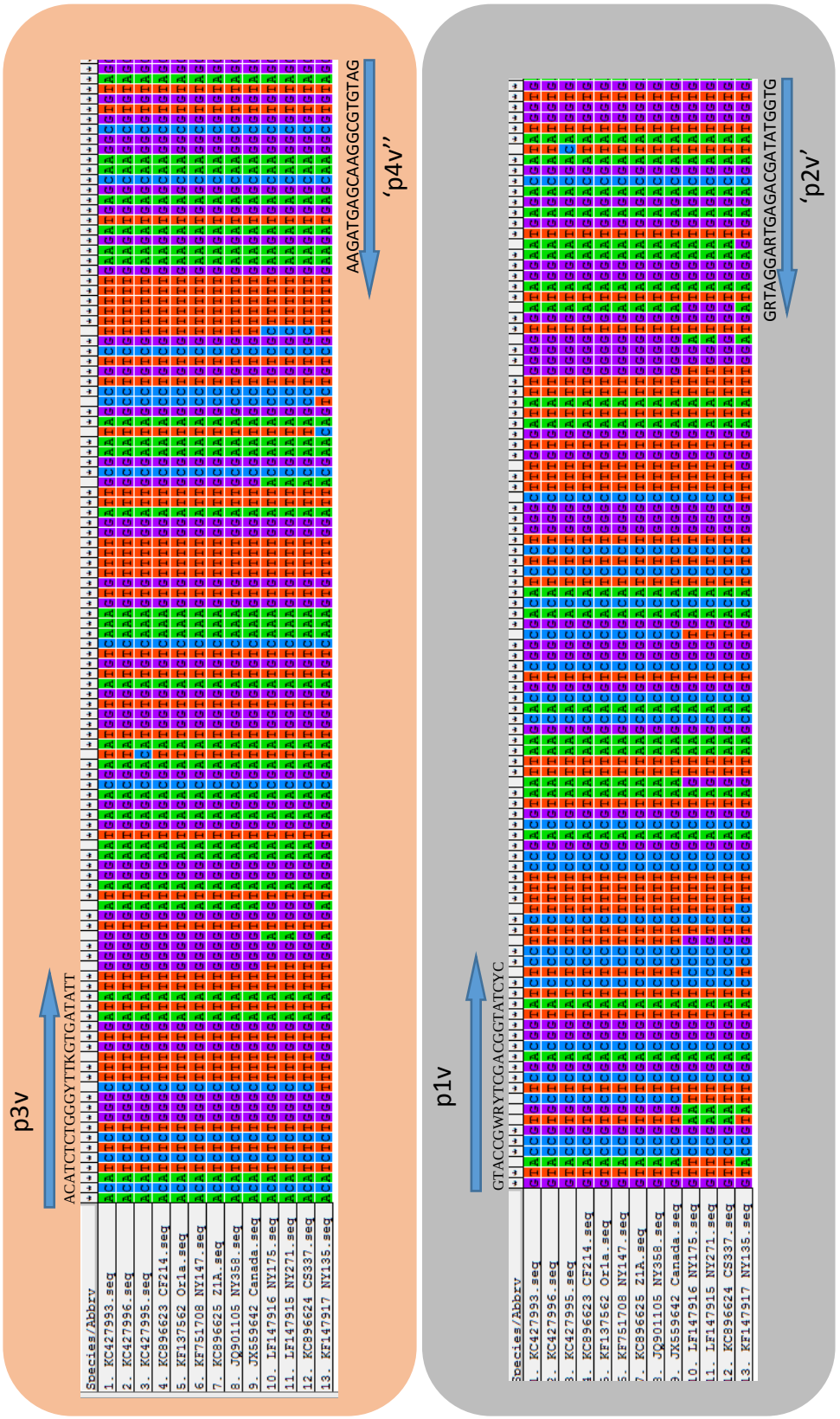

(b)

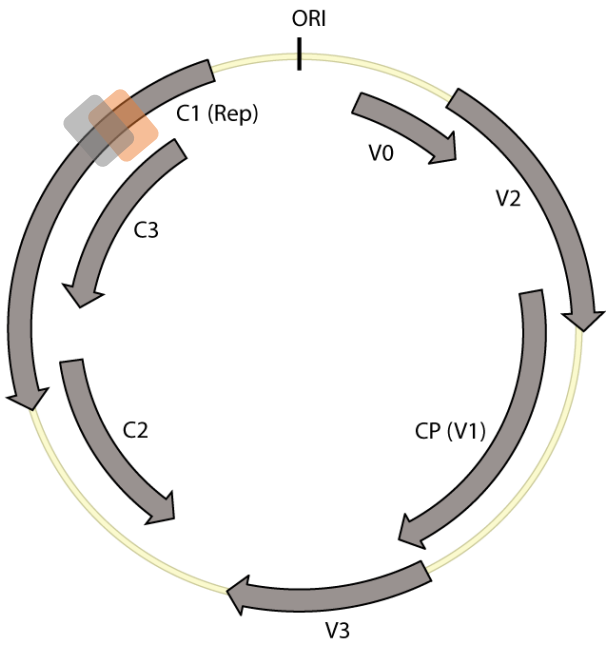

Figure 1. (a) Alignment of virus-specific primers corresponding to sequences between different GRBaV isolates. (b) Location of designed virus-specific primers on the GRBaV genome. Different color boxes correspond to distinct primer pairs. p1v, p2v, p3v, and p4v all refer to primer names listed in Table 1.

3. Validation of virus/internal control primer combinations.

Seven 2-fold dilutions of total nucleic acid (TNA) from GRBaV- infected tissue served as templates for qPCR. Each 25µl qPCR reaction contained 12.5 µl PerfeCTa® SYBR® Green FastMix® plusROX™ (Quanta Biosciences, MD, USA), 10.5 µl H_2O, 0.5 µl x µM forward primer, 0.5 µl x µM reverse primer, and 1µl of template TNA. All reactions were run in duplicate or triplicate in a thermocycler (ABI 7000 Sequence Detection System, Applied Biosystems, Waltham, MA, USA) with cycling conditions of 5 min 95°C (x1) and 30s 95°C, 30s 60°C (x40). Threshold cycle number (C_T) values were set automatically by the ABI PRISM® 7000 Sequence Detection System software V1.2x. C_T values data were exported and their averages and standard deviation calculated.

When C_T values between triplicates had a standard deviation >0.3, two data points were taken instead and unless the standard deviation of the two data points became <0.3, data points were not used as per recommendations by the MIQE guidelines (Hodzic 2011). Differences between the C_T values (ΔC_T) of the two primer pairs (virus specific and internal control) for each TNA dilution were calculated. Regression analysis was done for ΔC_T against the log amount of TNA input and the line of best fit was generated for ΔC_T. A slope of <0.1 was set as the acceptable threshold for equally efficient primer pairs (Applied Biosystems 2004). The overall process of choosing the set of virus specific and internal control primers is shown in figure 2.

In addition, PCR amplification efficiencies (E) were calculated based on the slope (m) of ΔC_T value against the log amount of TNA input using equation (1) (Yuan et al. 2006).

Efficiency formula: $$E = 10^{-\frac{1}{m}} - 1 \quad (1)$$

4. Determination of the reproducibility between qPCR experiments

The selected primer pair combination (virus specific and internal control) was further validated based on reproducibility in C_T values between independent assays. Several identical TNA input and primer pairs were run as above in three independent assays. C_T values for virus specific and internal control primers across different assays for each TNA input were averaged and the standard deviations calculated. Coefficient of variation (CV) calculation were subsequently made using equation (2), where 'σ' signifies sample standard deviation and 'μ' signifies sample mean.

Coefficient of variation formula: $$\boldsymbol{CV = \frac{\sigma}{\mu} \times 100} \quad (2)$$

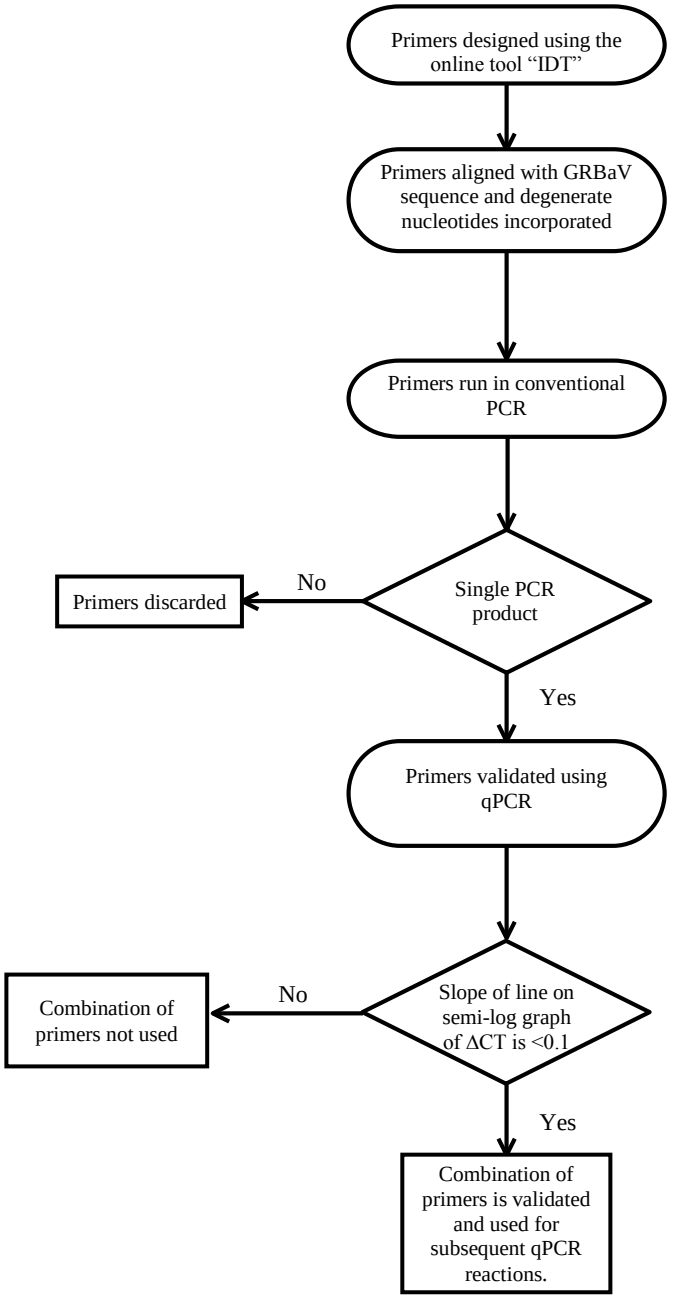

Figure 2. Flowchart showing primer selection process.

5. Plant samples

5.1 Greenhouse sampling

Plant tissues were sampled from greenhouse-grown *Vitis vinifera* 'Carbernet franc', located in the Yellow Greenhouse & Laboratory Complex, Cornell University Campus, Ithaca, NY 14853. Growth conditions were 16/8h (light/day) photoperiod at 22±3°C. Tissues collected included mature expanded leaves found at the basal and middle part of the cane, petioles of the respective leaves, and emerging leaves (1-3cm in length) taken from GRBaV-infected grapevines GV30, GV31, and GV32. Healthy grapevine from the clone TJB1-1 (Cabernet franc) was used for the negative plant controls.

5.2 Vineyard Sampling

Four field grown grapevines (R18V1, R18V19, R20V3, AND R20V9) of *V. vinifera* 'Cabernet sauvignon' from a commercial vineyard testing positive for GRBaV using a multiplex PCR method (Krenz et al. 2014) were selected for sampling in mid-June of 2015. Three canes of approximately 1.5m in length per plant were collected. For each cane, seven leaf and petiole samples were excised as shown in Figure. 3. Tissue samples were snap frozen in liquid nitrogen and stored at -80°C until TNA extraction.

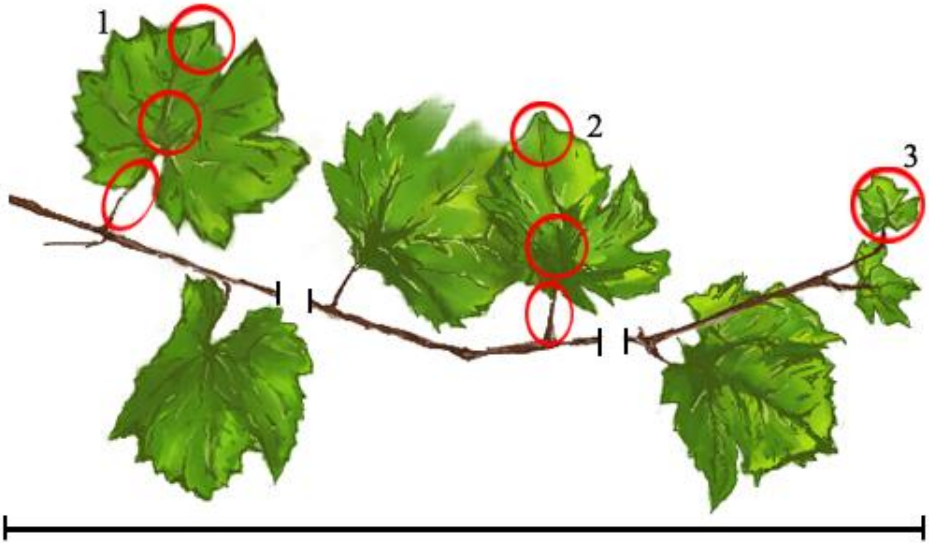

Figure 3. The relative positions along a grapevine cane that were sampled. Red circles indicate the parts of the vine that were excised and extracted. Two samples were taken from each location (red circle) for each vine, namely older leaf (1) petioles, basal and top part, intermediate leaf (2) petioles, basal and top part, and emerging leaf (3) entire leaf. Black bars indicate discontinuity along the cane in between the leaf tissues sampled.

6. External control preparation for absolute quantitation

Total nucleic acids from GRBaV-infected material was used as a template for rolling circle amplification using the TempliPhi™ amplification kit (GE Healthcare, UK) as described by the manufacturer. The amplification products were digested by *Pst*I (New England Biolabs, MA, USA) and separated by agarose gel electrophoresis. The virus specific fragment of 3.2kb was excised from the gel using the Zymoclean™ Gel DNA Recovery Kit (Zymo Research, CA, USA) and cloned into pUC19 linearized by *Pst*I. The resulting plasmid was propagated in *Escherichia coli* cells (DH5α) and purified using the EZNA plasmid midi kit (Omega, GA). The

concentration of the resulting pUC19MLV1.0 plasmid was determined spectrophotometrically (NanoVue Plus, GE Healthcare) and dilutions made accordingly.

7. qPCR

Extracted and normalized TNA from plant samples was used as the template for qPCR. Duplicates of all samples were run in parallel with either virus specific or internal control primers. Data on the amount of internal control input were used in each experiment to allow normalization of amount of virus relative to the amount of DNA added to the reactions. This ensured the calculated virus amount was not affected by experimental treatments (Livak and Schmittgen 2001). Additionally, a positive control and calibration standard of three 100-fold dilutions of previously prepared GRBaV plasmid (section 6) were run in duplicates for every assay. A negative control was also included in every assay in the form of RNase-free water. Cycling conditions are as stated in section 3. The C_T value thresholds for each reaction were set automatically by qPCR software (Applied Biosystems 2004) as well. C_T values were exported and their averages and standard deviations calculated.

8. Comparative C_T method ($\Delta\Delta C_T$) calculating fold change.

$\Delta\Delta C_T$ method was used to calculate fold difference (relative amounts) of virus DNA in a specific sample A compared to the amount in a second sample B (Yuan et al. 2006; Applied Biosystems 2004). Differences between the C_T values (ΔC_T) of the two primer pairs (virus specific and internal control) for each TNA sample were calculated.

$\Delta\Delta C_T$ was calculated by subtracting ΔC_T of sample B from ΔC_T of sample A (3), where sample A and B refer to individually extracted TNA sample from a specific tissue and plant. Fold difference was calculated using the formula $2^{-\Delta\Delta CT}$. This value indicates the amount of

target sequence found in sample A relative to sample B. All calculations were done in Microsoft® Excel.

$\Delta\Delta C_T$ formula : $\Delta C_{TA} - \Delta C_{TB}$ (3)

9. Absolute quantification

Average and standard deviation of C_T values for plasmid-derived GRBaV DNA were used for absolute quantification of GRBaV DNA found in extracted TNA samples. Regression analysis was done for C_T values against the log amount of copies of GRBaV plasmid input in the qPCR reaction. The line of best fit was generated for C_T and the log amount of GRBaV DNA. The equation generated for the line of best fit was used to calculate the absolute amount of the virus found in each sample (Feng et al. 2006; Yuan et al. 2006; Livak and Schmittgen 2001).

C_T values corresponding to extracted TNA of several known uninfected plants from repeated qPCR assays were also recorded. The corresponding number of viral copies was calculated using aforementioned regression analysis. The 95^{th} percentile of these values were set as the C_T value/viral copies cutoff.

A mixed effect model was used to analyze differences between the amounts of virus in different tissue types, taking into account the random effects potentially given by different plants, different canes within a plant, and different leaf developmental stages within each cane (i.e. older leaves and intermediate leaves). The mixed effect model is used when differences in fixed variables are potentially affected by sources of variations from one or more random variables (Piepho et al. 2003; Searle et al. 1992). The model also produces a more robust analysis when sample size is small, variances are unequal or unbalanced design of data is present (Savary and Cooke 2007). Tukey's HSD (honest significant difference) tests were done to evaluate significance in differences of virus concentrations between the tissue types. The significance

level was set at $\alpha = 0.05$. Model analysis was done in JMP® 12 Pro statistical software (© SAS Institute Inc., NC, USA).

Results

1. Virus-specific and internal control primer pairs were validated for use in a qPCR assay

Two virus-specific primer pairs, p1v/p2v and p3v/p4v, were designed from the GRBaV genome. Additionally, three internal control primer pairs were designed for use in normalizing virus expression data. The selection of gene targets for normalization was based on the work of Liu et al. (2012). Primer pairs targeted the following genes: Elongation factor 1-α (EF1α; GenBank accession NC_012014), NADP-dependent Glyceraldehyde 3-phosphate dehydrogenase (GAPDH; GenBank accession NC_012010) and Actin (ACT; GenBank accession NC_012014) (Table 1).

In order to ensure specificity of primers, each primer pair was tested with GV30 TNA as template using conventional PCR. Of these primer pairs, both virus-specific primer pairs and two out of three internal control primer pairs yielded a single PCR product of the expected size of approximately 110 bp (Figure 4.). Healthy grape controls were also free of any amplification product for all three virus specific primer pairs (not shown). Only primer pairs with specific products were used in subsequent experiments.

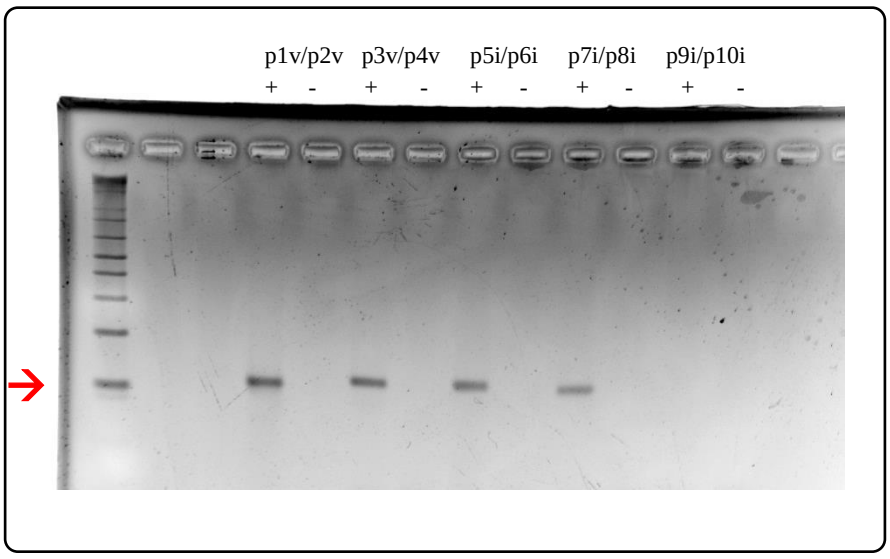

Figure 4. Agarose gel showing simplex PCR products from assays with virus-specific and internal control primer pairs. The primer pairs used are indicated above the respective lanes. Adjacent to and following each lane (indicated with +) is a water control for each of the corresponding primer pair (indicated with -). The red arrow indicates the position of a 100 bp molecular weight marker.

In order to develop a qPCR assay, one must ensure that the internal control primers have a comparable efficiency as that of the virus-specific primers (Applied Biosystems 2004). To validate the primers, each virus-specific primer pair was analyzed in combination with each internal control primer pair using qPCR. ΔC_T variations corresponding to changes in dilution of GV31 TNA template were plotted on a semi-logarithmic graph with log values of TNA dilutions input. (Figure 5.) The line of best fit drawn for each of the semi-logarithmic graphs and slopes of the lines are summarized in Table 2. Only the combination of p3v/p4v as virus-specific primer pair and p7i/p8i as internal control primer pair had a line of best fit whose absolute value of its slope was <0.1; this is the limit for which primer combinations are said to be equal in efficiency. (Applied Biosystems 2004)

Another criterion for the effectiveness of a qPCR assay is ensuring that PCR amplification efficiency is close to 1, meaning products are amplified exponentially during measurement of C_T values by the primers used. Primer combinations of p3v/p4v and p7i/p8i have PCR amplification efficiencies of 0.93 and 0.94 respectively, which are close to 1 (100% efficiency) (Bustin et al. 2009; Schmittgen and Livak 2008)

Table 2. Table listing the absolute value of slopes of semi-logarithmic graphs presented in Figure 5. and amplification efficiency of primer pairs in each primer pair combination assays.

Virus specific primer pair	Internal control primer pair	Absolute value of slope of line of best fit	Efficiency of virus specific primer pair	Efficiency of internal control primer pair
p1v/p2v	p5i/p6i	0.6799	0.78	1.01
	p7i/p8i	0.8227	0.81	1.12
p3v/p4v	p5i/p6i	0.3144	0.90	1.03
	p7i/p8i	0.0279	0.93	0.94

Primer combination p3v/p4v and p7i/p8i were used in subsequent qPCR assays since the combination passed the two required conditions for relative quantification using a qPCR assay.

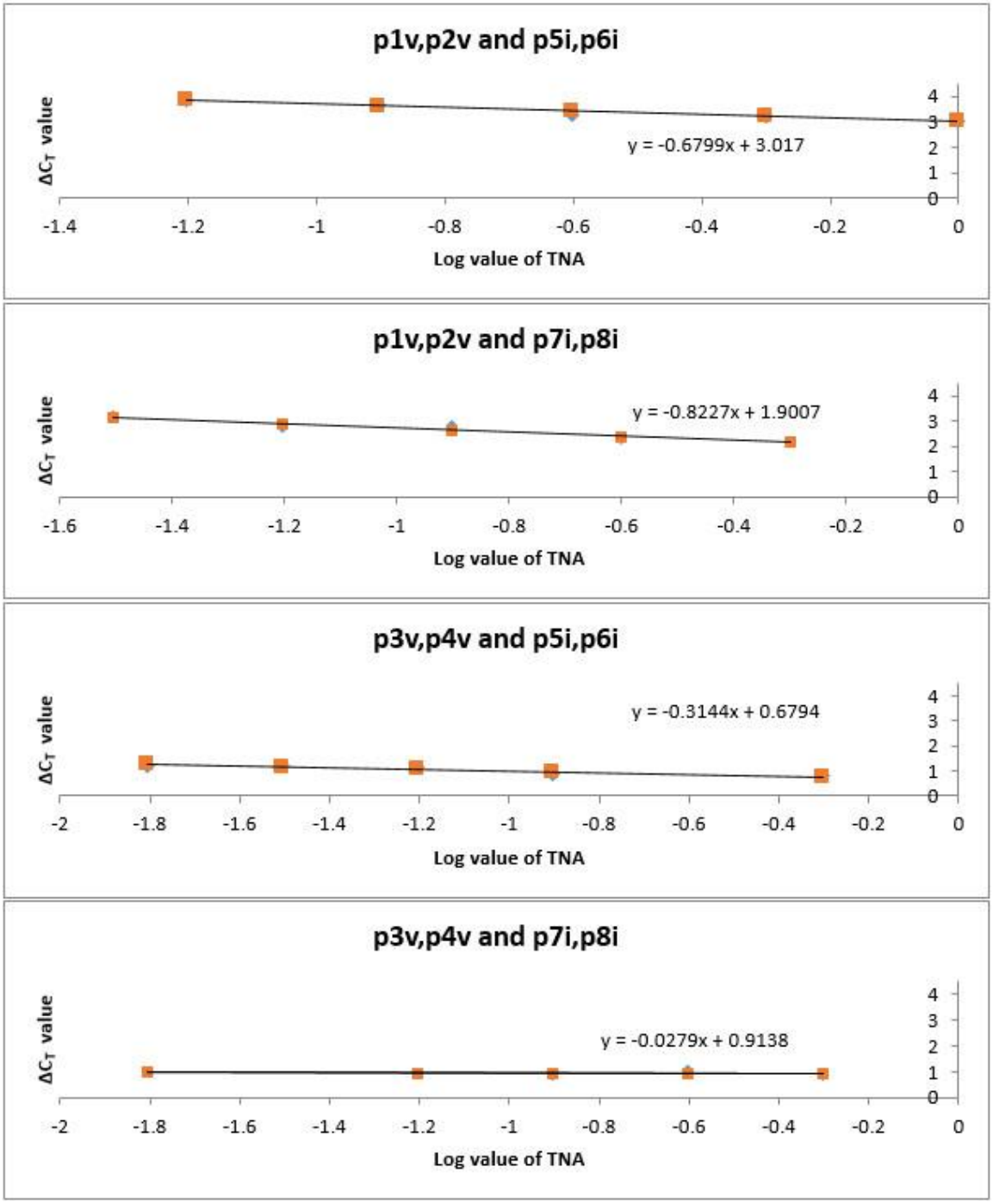

Figure 5. Semi-logarithmic graph of ΔC_T values and log input of TNA of GV31 for different combinations of virus specific primer pairs and internal control primer pairs. Blue diamonds indicate actual data and orange squares indicate expected data as estimated by the regression analysis. When the two overlap, only orange squares are seen.

2. qPCR assay is highly reproducible across samples and time points

In order to assess the reproducibility of the assay, the coefficient of variation (CV) for average C_T values across independent assays was calculated. Average and standard deviation of C_T values were obtained from at least three independent assays. Each assay used three dilutions of extracted GV31 TNA as templates containing 200, 100, and 50 ng/µl of TNA respectively. The experiment was also repeated twice using different GV31 TNA as templates (different GV31 TNA are labeled as sample A, B, and C as collected from three different canes). Average C_T values and CV are summarized in Table 3.

Table 3. Table showing average C_T values and corresponding CV for validated virus specific and internal control primer pairs from independent assays using dilutions of GV31 TNA as templates.

Primers pairs used		p3v/p4v		p7i/p8i	
Sample	TNA concentration (ng/µl)	Average C_T	CV (%)	Average C_T	CV (%)
A	200	22.376	2.03	23.721	1.36
	100	23.629	1.26	24.545	1.15
	50	24.704	1.86	25.850	1.25
B	200	22.887	1.78	23.845	1.32
	100	24.133	1.13	24.860	1.35
	50	25.355	1.37	25.980	1.42
C	200	20.672	1.75	25.203	0.92
	100	21.777	1.81	26.317	1.27
	50	23.077	1.57	27.180	1.19

CV of the average C_T values in three dilutions of GV31 TNA were minimal (Pfaffl 2001). The highest value for the previously validated virus-specific and internal primer pairs are 2.03% and 1.42% respectively.

3. GRBaV copy numbers in different tissue types of a single greenhouse grown plant are very similar.

To assess whether concentrations of GRBaV differ between different tissues of one plant, 11 canes were sampled from a single GV30 plant and TNA was extracted from the petiole, basal, and top part of an old leaf. TNA was also extracted from an emerging leaf from each cane. The extracted TNA preparations were used as templates and tested by qPCR using the previously validated primer pairs (p3v/p4v and p7i/p8i).

Comparison of viral concentration in different tissues was done using absolute quantification through regression analysis of an external control; C_T values of dilutions of isolated GRBaV plasmid were plotted on a standard curve and line of best fit was subsequently used to quantify the GRBaV concentration in each sample. The starting concentration of the GRBaV plasmid was 6ng/µl. Subsequent hundred-fold dilutions of GRBaV plasmids had concentrations of 60 pg/µl, 600 fg/µl, 6 fg/µl, and 60 ag/µl. This corresponds to 10^9, 10^7, 10^5, 10^3, and 10 copies of the GRBaV plasmids.

Two TNA samples from uninfected plants were run in three qPCR assays along with the GRBaV plasmids and water controls. The lower threshold of detection average was 3.49×10^3 copies and the 95^{th} percentile is 6.81×10^3 copies. The latter was set as the cutoff value; in subsequent experiments values below the cutoff were regarded as negative for GRBaV. Instead of stating these values contain zero viral copies, a value of 0.05 copies was specified to allow for presentation and analysis of log values of viral copies.

The number of viral copies for each tissue type from 11 GV30 canes was averaged and plotted on a bar graph (Figure 6.)

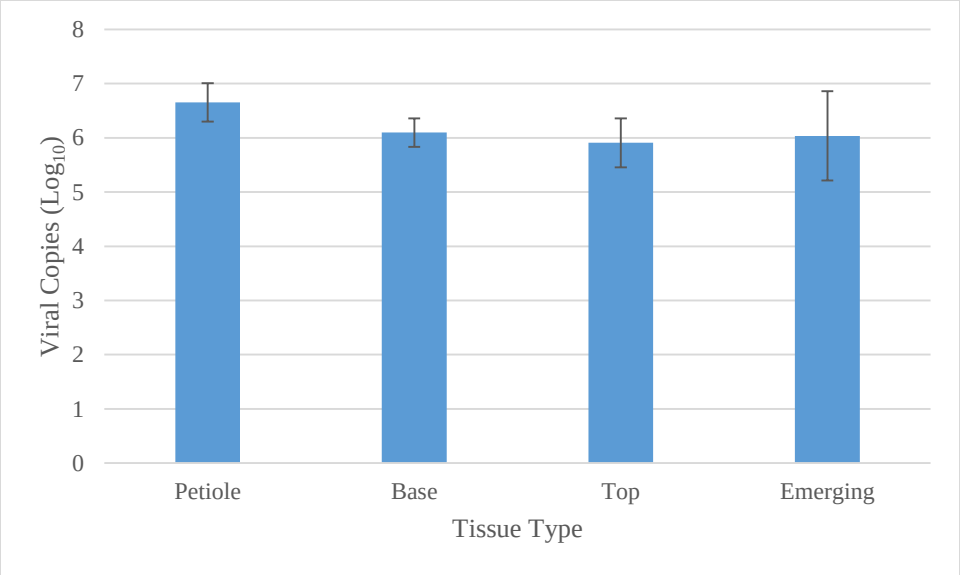

Figure 6. Bar graph showing the average log value of viral copies in extracted TNA of different tissue types in GV30. Error bars show standard error of the mean.

Kruskal-Wallis test revealed that the mean number of viral copies in the petiole of 4.47 x 10^6 is significantly different than that in the basal part of a leaf of 1.25 x 10^6 (P=0.03); no differences were observed among the other tissues.

4. GRBaV copy numbers in greenhouse-grown plants vary between tissue types

In quantifying the GRBaV concentration in infected host plants, two different quantification approaches can be used, namely absolute and relative quantification. Absolute quantification directly uses reported C_T values converted to viral copies using an external control (GRBaV plasmid in this case). Relative quantification on the other hand normalizes virus concentration against concentration of an internal control to ensure quantification of GRBaV in different samples is not confounded by differences in initial concentration of DNA used as templates or PCR inhibitors.

In greenhouse-grown *V.vinifera*, the virus concentration in different tissues of plants was quantified to assess the variability of virus levels between plants. Tissues from greenhouse-grown plants sampled were collected from canes of plants GV30 (n=3), GV31 (n=3), and GV32 (n=4) for a total of ten canes; each of these plants were clonally propagated in 2012 from the same original mother vine.

The resulting virus copy numbers were calculated using regression analysis of external controls, averaged and are plotted on a bar graph (Figure 7.)

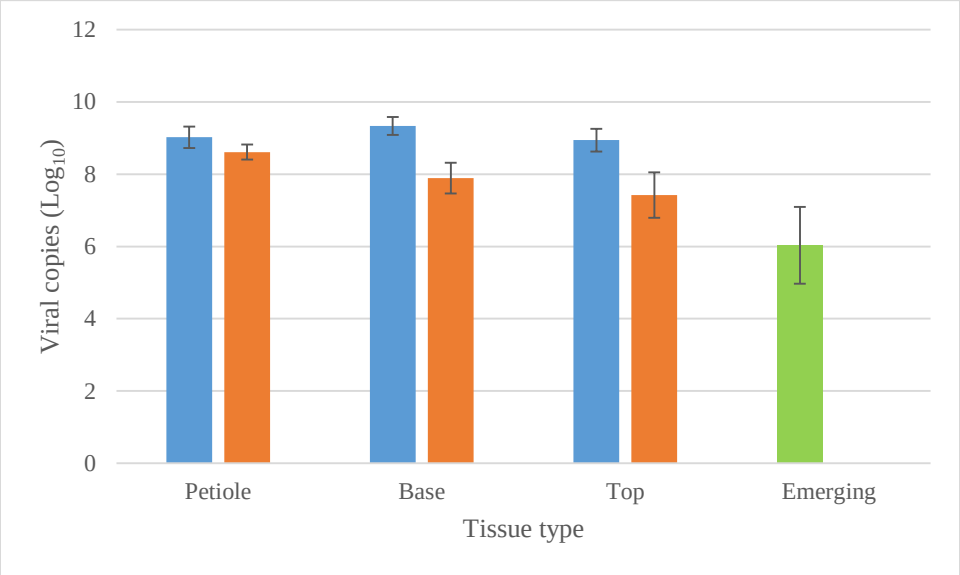

Figure 7. Bar graph showing the average log number of viral copies in extracted TNA of different tissue types in ten canes collected from three greenhouse-grown plants. Blue bars indicate viral copies found in old leaves, orange bars indicate those found in intermediate leaves, and green bar indicates those found in emerging leaves. Error bars show standard error of the mean.

A mixed effect model was used to identify significance in differences of virus amount in different types of tissues (petiole, and basal, and top leaf samples). As aforementioned, the model was used because it takes into account the random effects from differences in plants, canes, and

leaf developmental stages (old leaf and intermediate leaf), allowing for a more accurate analysis of the differences in virus amount across tissue types. The fixed effect test within the model revealed that there were no significant differences in viral concentration between petiole, base, and top part of a leaf in greenhouse-grown plants.

However, it can be observed from Figure 7 that there are potential differences in the pattern of virus concentration between different tissue types in the old and intermediate leaves. The statistical analysis was thus repeated for both old leaves and intermediate leaves independently. The Tukey's HSD test revealed that there was in fact a significant difference between amounts of GRBaV in petiole compared to that in the top part of intermediate leaves. ($P<0.04$) This difference is not significant in old leaves.

Further tests were done to measure overall virus amount in the old, intermediate, and emerging leaves. Virus copy numbers in old and intermediate leaves were obtained by averaging the data for petioles and the corresponding basal and top part of the leaves. After taking into account the potential random effects from different plants and canes, Tukey's HSD tests revealed that the virus amount between old leaves and emerging leaves, as well as between intermediate leaves and emerging leaves are significantly different ($P<0.01$and $P<0.03$ respectively).

Relative quantification was done to assess the extent of the differences in virus concentration in different tissue types from greenhouse-grown vines after normalization to the level of detection of an internal control gene. The $2^{-\Delta\Delta CT}$ method was used and results are plotted on figure 8.

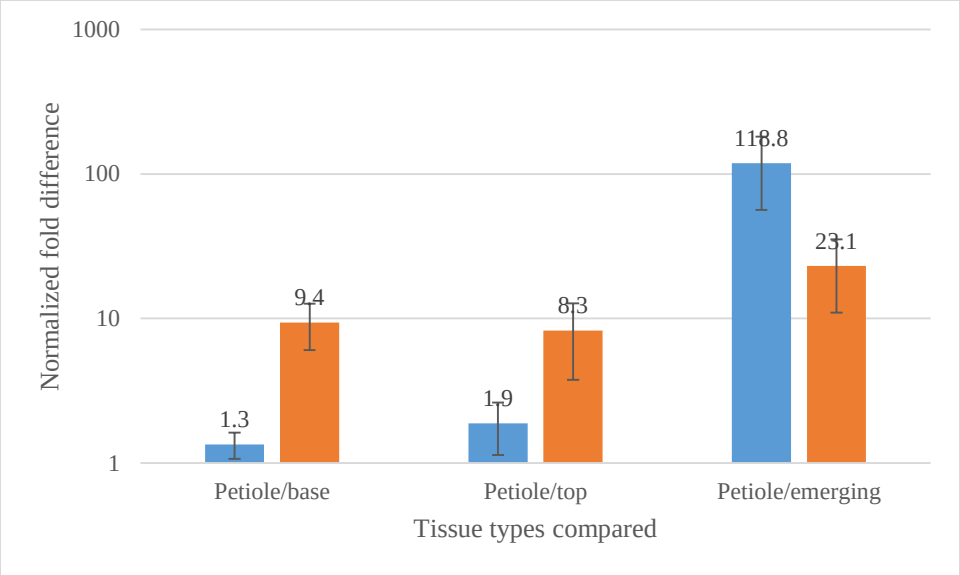

Figure 8. Bar graph showing the fold difference of GRBaV amount in petiole compared to other types of tissues in greenhouse-grown vines. Vertical axis is set on logarithmic scale. Error bars indicate standard error of the mean. Petiole/base signifies amount of GRBaV in petiole relative to base part of leaf. A value greater than one indicates that GRBaV amount is higher in petiole than in the tissue type being compared to it. Blue bars indicate results for old leaves, while orange bars indicate results for intermediate leaves.

Concentration of GRBaV in the emerging leaf is much lower when looking at samples from several greenhouse-grown plants (as opposed to only GV30 plants). This is confirmed with a large fold difference in the amount of GRBaV found in the petioles of older leaves in comparison to that found in emerging leaves (on average, 118.8 times more).

5. GRBaV copy numbers in field-grown plants vary between tissue types

Virus concentration in different tissues of field-grown *V. vinifera* was also assessed. A total of 12 canes were used as a source of TNA (4 plants, 3 canes per plant). Absolute and relative virus amounts are shown in figure 9 and figure 10, respectively

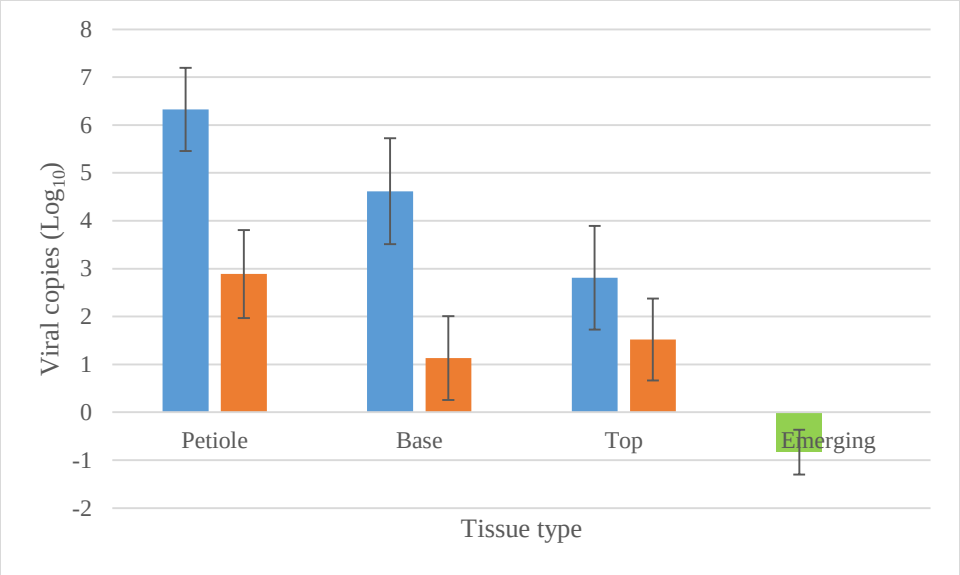

Figure 9. Bar graph showing the average log number of viral copies in extracted TNA of different tissue types in four field-grown plants. Blue bars indicate viral copies found in old leaves, orange bars indicate those found in intermediate leaves, and green bar indicates those found in emerging leaves. Error bars show standard error of the mean.

In general, viral copies detected in field-grown plant samples were lower than viral copies detected in greenhouse-grown plants. The distribution and concentration of virus in field-grown plants is strikingly different from that in the greenhouse-grown plants in that most of the emerging leaves tested negative for GRBaV. (Figure 9.)

As above, a mixed effect model was used to test for significance in differences of virus amount between different tissue types (petiole, basal, and top part of a leaf), while taking into account random effects due to differences in plant, cane, and leaf developmental stages (old leaf and intermediate leaf). The model revealed that differences in virus amount between tissue types is significant ($P<0.01$). Tukey's HSD tests further revealed that the significance in the model is due to significant differences in virus amount found in the petioles compared to the top part of leaves ($P<0.01$).

Figure 9 also shows potential differences in the pattern of virus amount across tissue types between the old leaves and the intermediate leaves. When the same statistical analysis was repeated for old leaves and intermediate leaves independently, it is revealed that there are significant differences in the amount of virus between the petiole and top part of leaves in old leaves, but not for intermediate leaves. ($P<0.01$)

As previously done, virus amount in the old leaves, intermediate leaves, and emerging leaves were tested. After taking into account the potential random effects from different plants and canes, Tukey's HSD tests revealed that there are significant differences in the virus amount between old, intermediate, and emerging leaves. (Table 4.)

Table 4. Table listing p values for mean differences in log of copy numbers of virus found in old leaves, intermediate leaves, and emerging leaves within a single cane.

Leaf developmental stage (position in the cane)	Old leaves	Intermediate leaves	Emerging leaves
Old leaves		<0.02	<0.0001
Intermediate leaves			<0.01
Emerging leaves			

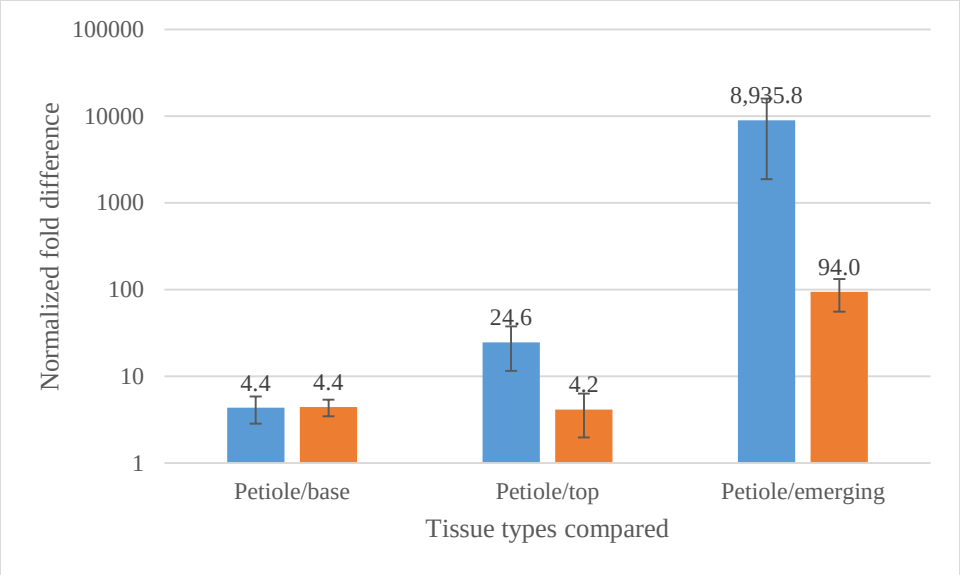

Figure 10. Bar graph showing the fold difference of GRBaV amount in the petiole compared to other types of tissues in field-grown plants. Vertical axis is set on logarithmic scale. Error bars indicate standard error of the mean. Error bars indicate standard error of the mean. Petiole/base signifies amount of GRBaV in petiole relative to the leaf base. A value greater than one indicates that the GRBaV amount is higher in petiole than in the tissue type being compared to it. Blue bars indicate results for old leaves, while orange bars indicate results for intermediate leaves.

As can be observed, petioles seem to be where the highest amounts of GRBaV are observed as similarly found in greenhouse-grown plants. The extent of the difference in virus amount in different types of tissues is however not the same for greenhouse-grown plants and field-grown plants. For example, there is 94 times more GRBaV in TNA extracted from the petiole (of an intermediate leaf) compared to that from the emerging leaf in field-grown plants as opposed to only 23 times more GRBaV found in the greenhouse-grown plants.

6. GRBaV copy numbers in different tissues vary between greenhouse- and field- grown plants.

The proportion of samples that were regarded as negative for both greenhouse- and field-grown samples were calculated and presented as percentages of samples obtained for each tissue type. (Table 5.)

Table 5. Percentages (%) of samples regarded as negative by set cutoff value for all tissue types in different leaf types and growing locations (greenhouse- and field-grown).

Leaf type	Old leaves			Intermediate leaves			
Tissue type	Petiole	Base	Top	Petiole	Base	Top	Emerging
Greenhouse-grown plants	0	0	0	0	0	0	11.11
Field-grown plants	8.33	25.0	41.67	33.33	58.33	50.0	91.67

As can be observed, many field-grown samples yielded a lower virus amount compared to greenhouse-grown samples; a higher percentage of samples from field-grown plants were tested negative for GRBaV. Moreover, negative samples were found more in younger leaves (intermediate and emerging) compared to in older leaves. The variations in GRBaV copy numbers in different tissue types between greenhouse- and field-grown plants can also be observed when all GRBaV copy numbers in different tissue types are plotted against the corresponding plant and canes (Figure 11.)

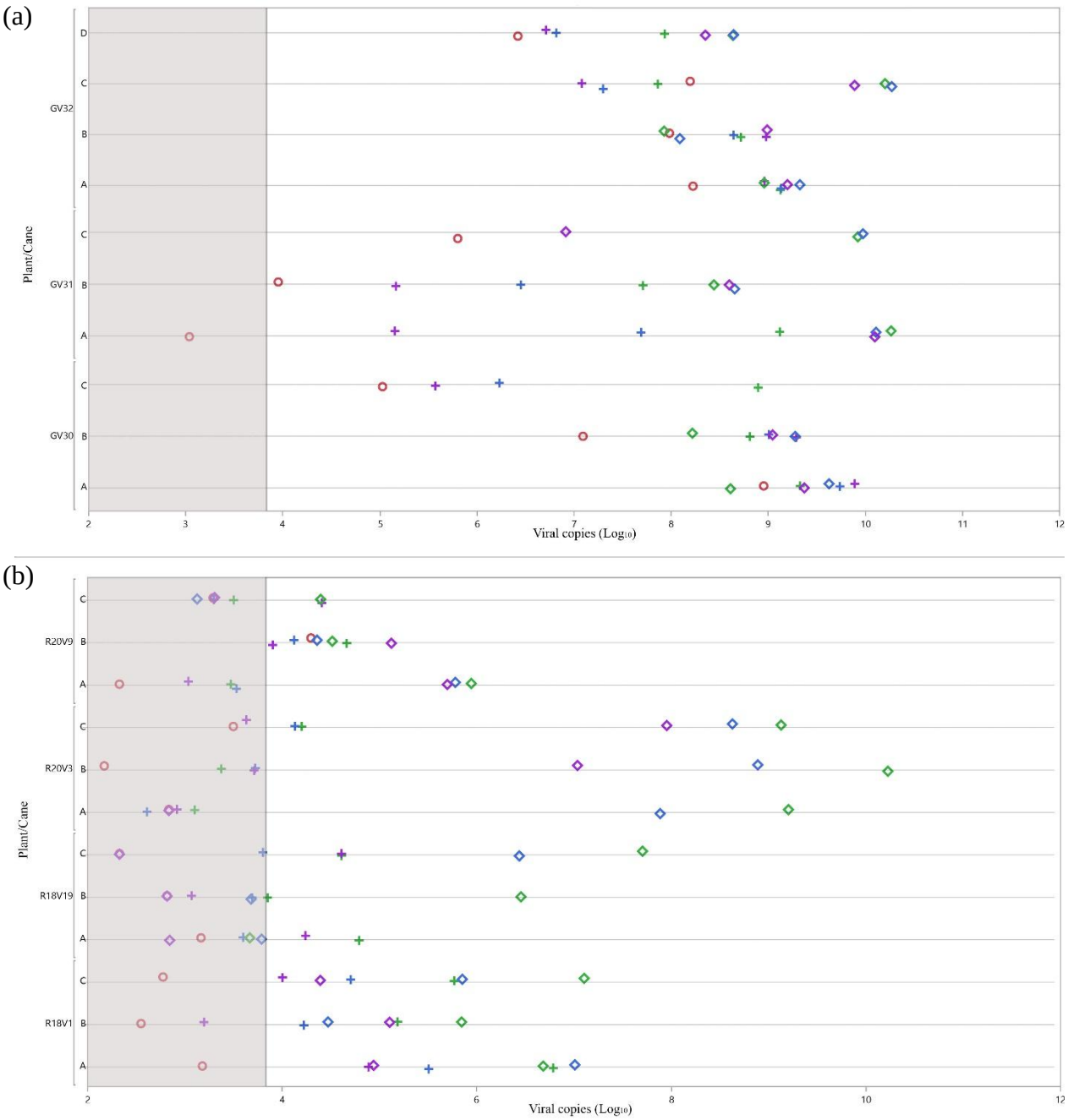

Figure 11. Plotted GRBaV viral copy numbers (Log values) for greenhouse- (a) and field-grown plants (b). Green, blue, purple, and red correspond to petiole, basal, top, and emerging leaf data points. Diamond (◇), cross (✚), and circle (○) correspond to old, intermediate and emerging leaves data points respectively. Data points located in the grey areas are below the cutoff value and were regarded as negative.

7. Measurements of virus concentration using external controls (absolute quantification) versus internal controls (relative quantification) provide comparable results

Since the initial concentrations of TNA in all samples used in qPCR analysis were adjusted to 50ng/µl, it was assumed that the initial concentration of internal control gene is similar in all templates. Subsequently, comparison of absolute values of viral copies can be used to evaluate the extent of differences in virus concentration in different tissues without analysis of differences in the amount of internal control gene in initial TNA templates. Relative quantification on the other hand, requires one to compare differences in virus C_T values in different tissues by normalizing virus C_T values against the C_T values of the internal control gene. This allows adjustments which should mitigate inaccuracies due to differences in the actual starting DNA concentration; extracted TNA contains both RNA and DNA in the infected host plants and actual proportion of DNA in TNA could not be precisely assessed.

Consequently, a scattered plot showing the correlation between the proportion of viral amount to internal control gene amount from the two quantification methods (relative and absolute) was done to evaluate the consistency between relative and absolute methods for GRBaV quantification. The plots were done for both greenhouse-grown plants and field-grown samples are shown in Figure 12 (a) and (b) respectively.

(a)

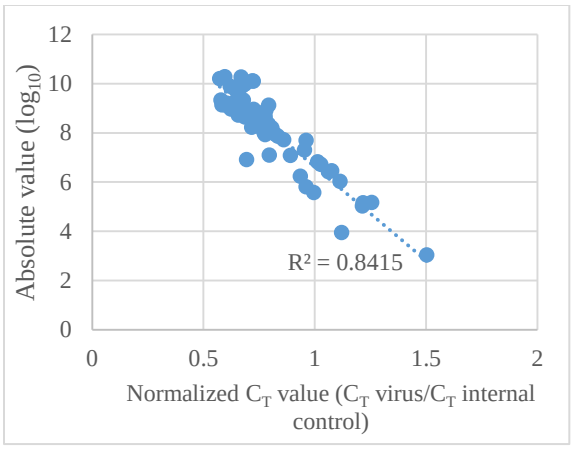

(b)

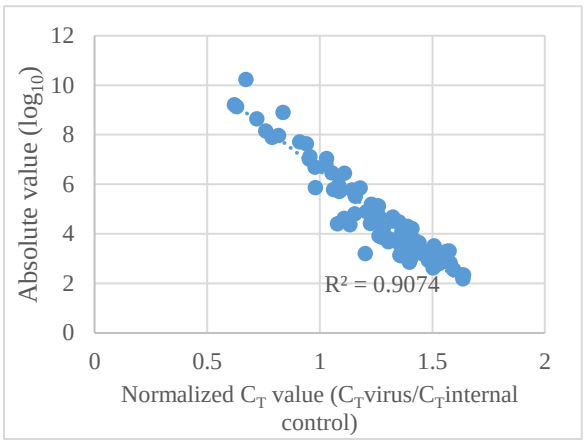

Figure 12. Scattered plots of normalized GRBaV expression (Virus DNA amount compared to internal control DNA amount) in (a) sampled greenhouse-grown plants and (b) sampled field-grown plants.

There is a strong correlation between the results obtained from absolute and relative quantification. However, the correlation is weaker in greenhouse-grown plants than in field-grown plants. Weaker correlation signifies that the validity of the results obtained from absolute quantification in greenhouse-grown plants may be undermined by the fact that there are substantial differences in the initial total DNA concentration added to the reaction. This difference would be represented by differences in the expression level of internal control gene in different samples.

Discussion

This study presents the development and application of a quantitative assay for GRBaV detection in grapevine using qPCR. Primers specific to GRBaV and grapevine GAPDH were validated for qPCR use. The two primer pairs selected were shown to fulfill several criteria necessary for virus quantification analysis; the two primer pairs have equal efficiencies, behaving similarly in response to differences in concentration of initial target sequences, and

PCR amplification efficiencies for both primers were close to 100%. The primers' efficiency was also shown to be repeatable across different assays, allowing accurate and consistent analysis of independent samples in independent assays. The qPCR assay was also able to detect GRBaV concentration as high as 10^9 copies and as low as around 10^3 copies. All of the above characteristics allow for both relative and absolute quantification of GRBaV in future diagnosis and detection studies.

A strong correlation between results derived from absolute and relative quantification also demonstrates that both methods can be utilized in future GRBaV diagnosis studies. However, due to inherent variability in the proportion of DNA in extracted TNA from infected plants, the use of internal control primers in the qPCR assay has distinct advantages over an absolute approach when assessing amounts of GRBaV. Geminivirus DNA has a number of replicative forms, from single stranded circular to double stranded linear (Erdmann et al. 2010). Removal of RNA using RNases was considered, but without a full understanding of the contributions of each DNA form during infection and their possible sensitivity to RNase treatment, using a standard amount of TNA was favored.

The qPCR assay confirmed that all sampled plants were GRBaV-infected, confirming previous diagnosis of the virus by Krenz et al. (2014). The assays also revealed that the pattern of virus concentration in different plants and different tissue types is variable; an observation that confirms anecdotal evidence of diagnostic inconsistencies from our lab and Marc Fuchs lab in Geneva where conventional PCR assays for the detection of GRBaV are routine.

When looking at only GV30 plants, emerging leaves had a similar amount of virus as older leaves regardless of the tissue type. However, upon sampling other plants grown in both the greenhouse and field, absolute quantification revealed that emerging leaves consistently

contain significantly lower amounts of GRBaV when compared to older leaves $P< 0.01$ and $P<0.0001$ for greenhouse- and field-grown plants respectively . A higher proportion of emerging leaves tested negative for GRBaV than any other tissue type (11.11% and 91.67% for greenhouse- and field-grown plants respectively).

Several findings were consistent across different plants grown in different locations. For example, in both greenhouse- and field-grown plants, petioles were found to contain significantly higher amounts of GRBaV when compared to the corresponding top parts of leaves. This result is confirmed by relative quantification, which consistently showed that GRBaV amounts in petioles are higher than in any other tissue type (basal, top part of the leaf and emerging leaves). A lack of significant differences in absolute GRBaV concentration between the basal part of the leaf and the petioles qualifies the former as potential tissue candidate to be routinely sampled; however, the basal part of the leaf did not prove to contain significantly higher amounts of GRBaV than other tissue types. Moreover, a large number of samples from the basal part of leaves of field-grown plants tested negative for GRBaV despite positive detection of the virus in the corresponding petioles (Table 5). Sampling basal and top part of leaves, as well as emerging leaves could result in increased risk of false-negative results. Consequently, for the most definitive detection of GRBaV, the petiole is the most suitable tissue type for diagnosis of GRBaV in potentially-infected plants.

The higher virus amounts found in petioles, organs closest to the cane and main stem, is consistent with the known mode of transport of other geminiviruses within their host. GRBaV is thought to be transmitted by leafhoppers like some other geminiviruses (Sudarshana et al. 2015). A previous study has reported the transmission of GRBaV by the Virginia creeper leafhopper (*Erythroneura ziczac* Walsh) under experimental conditions (Poojari et al. 2013). The virus has

also been shown to be transmissible by propagation and grafting methods. It is thus, generally accepted that GRBaV is a phloem-limited virus like many other geminiviruses (Krupovic, et al. 2009; Rojas et al. 2005). Phloem-limited viruses are often associated with a source-to-sink type of movement; viruses travel from site of infection to the main phloem vasculature and subsequently to sinks through bulk passive transport (Hipper et al. 2013). GRBaV-infected plants have been found to contain higher amounts of starch and sucrose in leaves and reduced total soluble solutes and anthocyanins in berries compared to their non-infected counterparts. This aberration in the allocation of sugar and related compounds potentially represents virus-associated disruptions of the plant's normal source-sink activity as the virus travels through the phloem of infected tissues (Poojari et al. 2013). A similar pattern of virus localization as found in this study has been observed in previous studies with other grapevine viruses such as *Grapevine leafroll-associated virus-3* (GLRaV-3) (Charles et al. 2006) and *Grapevine fanleaf virus* (Krebelj et al. 2015). Highest virus concentration was reported in basal (older) rather than apical (emerging) leaves (Teliz et al. 1987; Krebelj et al. 2015; Tsai et al. 2012). This is not surprising since the direction of phloem sap transport from source to sink (older to younger leaves) would initially result in higher virus titers in the basal rather than the apical part of canes. Other studies have also shown higher GLRaV-1, 2, and 3 concentrations were found in petiole samples and basal leaves compared to young leaves (Ling et al. 2001; Monis and Bestwick 1996).

Variability in the pattern of virus concentration between tissue types could additionally be attributed to differences in the initial site of infection between different plants as well as temporal and seasonal effects. In fact, the severity of blotches in GRBaV-infected plants, a symptom associated with the presence and spread of the virus, also varies between different cultivars and growing seasons (Sudarshana et al. 2015). In greenhouse-grown plants, a

significant difference in virus amount between the petioles and the top part of the leaves was found only in intermediate leaves (sampled from the middle of canes), and not in old leaves (sampled from the basal part of canes closest to the main stem). Emerging leaves from greenhouse-grown plants were also found to contain higher amounts of GRBaV as compared to those in field-grown plants. This indicates that in greenhouse-grown plants, a more advanced movement of GRBaV towards younger developing tissues has occurred. The old leaves appear saturated with the virus and differences in virus concentration between tissue types in old leaves are negligible. In field-grown plants however, a significant difference in virus amounts between petioles and the top part of leaves was found in old leaves. This suggests that GRBaV in field-grown plants is still mostly localized within tissues closest to the main stem. This is further confirmed by significant differences found in overall virus amounts between old leaves, intermediate leaves, and emerging leaves.

The differences between greenhouse-grown plants and field-grown plants are not surprising, considering the different growing conditions of the two groups of plants. While the greenhouse-grown plants are occasionally exposed to cold treatments, they were mostly grown at a constant 22±3°C. Field-grown plants on the other hand are exposed to more drastic temperature changes according to seasonal changes, potentially limiting virus replication and movement to the growing seasons. Movement of solutes from leaves and active sinks to reserves (canes and roots) is associated with low temperatures and the end of the growing season (Loescher et al. 1990; Lemoine et al. 2013). If GRBaV is truly phloem-limited, such physiological behavior will constrain GRBaV spread to younger leaves which are usually active sinks. This allows for more extensive virus movement and spread throughout the canes of greenhouse-grown plants compared to that of field-grown plants. Seasonal fluctuations effects on variations in pattern of

virus concentration in different tissue types and leaves at different cane positions have also been reported in other studies. Virus localization study on GLRaV-1 and -3 reported that differences in virus concentrations between older and younger leaves were only observed early in the growing season; at the end of the growing season, the virus concentration in the two types of leaves were comparable (Monis and Bestwick 1996). Similarly, differences in virus concentration between fully developed (older) leaves and emerging leaves observed in this study may no longer be observed in the future as movement of virus from older leaves to emerging leaves occur, as expected of bulk flow transport of the virus from source to sink. Other studies analyzing seasonal fluctuations of other grapevine viruses have also demonstrated that virus titers in young (apical) leaves can become significantly higher than in mature leaves as the growing season progresses (Krebelj et al. 2015; Tsai et al. 2012). Future studies regarding the seasonal fluctuations of GRBaV titers across different tissue types and leaves within a cane should therefore be conducted. Seasonal fluctuations of GRBaV titer will significantly affect sampling recommendations for accurate GRBaV detection and diagnosis. Decline in GRBaV concentration in older leaves may be observed as the growing season progresses (Krebelj et al. 2015); yet this study currently demonstrates that older leaves contain significantly higher amounts of GRBaV compared to younger and emerging leaves.

Other factors that could have contributed to variability in GRBaV amount between different plants grown in different locations include climatic conditions and GRBaV interactions with other viruses, vectors, and host plants (Mansoor et al. 2003; Maree et al. 2013; Chooi et al. 2016). Climatic conditions have been shown to have a significant impact on localization and expression of grapevines viruses (Constable et al. 2013). Higher temperatures during the growing season have been predicted to result in slower virus movement and rate of replication of viruses

associated with leafroll and fleck disease (Constable et al. 2013). Virus concentration also varies depending on incidence and frequency of infection. Virus detection studies across multiple seasons revealed a higher proportion of positive results for several grapevine viruses in samples taken in later seasons (Constable et al. 2012; Teliz et al. 1987). Field-grown plants are also extremely susceptible to multiple infections from several types of grapevine viruses. Mixed infections could result in fluctuations of virus titer and expression within host plants (Krebelj et al. 2015), thus multiple and repeated samplings are recommended to reduce the risk of false-negatives in GRBaV detection efforts.

There is higher variability in GRBaV amount within similar tissue types in field-grown plants compared to greenhouse-grown plants. This could be attributed to uneven distributions of GRBaV in plants, which is likely to be more prominent for plants grown in the field (Tsai et al. 2012). Overall, higher virus titers were found in greenhouse-grown plants than in field-grown plants. In fact, a large number of field-grown plants tested negative for GRBaV despite positive detection of the virus either in other canes or other tissues within a plant. Negative samples were determined by cutoff levels set by qPCR analysis of TNA from two non-infected plants which may have resulted in a skewed (and more conservative) cutoff value. It is thus recommended that an increased number of independent TNA samples from non-infected grapevines should be tested in qPCR in the future and cutoff values be revised as needed.

The ability to accurately and rapidly diagnose GRBaV in field-grown grapevines is important in preventing the spread of associated red blotch disease to new vineyards. GRBaV has mostly been isolated in the North American region, but recently GRBaV was reported on grapevine in South Korea and its sequence deposited in Genbank (Accession KU821056.1, unpublished data 2016). Increased global trade including the movement of plant materials across

continents has made virus spread across long distances feasible (Rojas et al. 2005). Reliable detection of GRBaV will contribute to GRBaV containment and red blotch prevention by ensuring the use of clean, virus-free rootstocks and scions in establishing new vineyards. Accurate detection will also allow for faster management in the case of confirmed infected plants in a vineyard and faster identification of potential sources of infection. In addition to economic losses, transmission of GRBaV into new locations also potentially increases the risk of the emergence of new opportunistic viruses and the transmission of GRBaV to novel species – as yet there is no information on the host-range of GRBaV. As mentioned, recombination between geminiviruses has been observed and can easily give rise to new viruses adapted to new ecological niches and new crops (Rojas et al. 2005); in fact new diseases associated with geminiviruses are already emerging in crops such as tomato, tobacco, chilies and papaya (Mansoor et al. 2003). Circular single-stranded DNA satellites and replicating components associated with geminiviruses, important for virus replication and maintenance of diseases, are believed to have adapted for increased transmission efficiency (Stanley et al. 2005) and host-range adaptation and diversification (Mansoor et al. 2003).

In conclusion, this study has demonstrated the establishment of an optimized detection method for GRBaV diagnosis allowing for both absolute and relative quantification of GRBaV. Samples of potentially-infected host early in the growing season should be obtained from petioles in older leaves, close to the main stem. As the growing season progresses, sampling can be extended to petioles of younger leaves, although the recommendation should be confirmed with future experiments investigating seasonal-associated fluctuations in GRBaV titer. The use of extremely young leaves found in the apical part of canes (emerging leaves) as sampling tissue should be avoided as a majority proved to give false-negative results for presence of GRBaV in a

plant. It is however, important to note that 8.3% of petioles sampled in old leaves failed to show positive detection of GRBaV in infected field-grown plants. Additionally, GRBaV distribution and accumulation in a plant can vary between different canes. Thus, to ensure accurate GRBaV detection in potentially-infected plants, it is recommended that several petioles from older leaves located in the basal part of several canes of one plant are sampled repetitively within and across different seasons to circumvent potential effects of seasonal fluctuations in virus titers and reduce risk of false-negatives results.

Acknowledgement

I would like to thank both Drs. Jeremy Thompson and Keith Perry for the extensive knowledge they have given me ever since I started working in the lab. I especially thank Dr. Jeremy Thompson for walking with and mentoring me throughout this whole project; helping me and keeping me calm throughout the multitude of trouble-shooting attempts and revisions that had to be made during the project. I would also like to thank the rest of the lab members who have contributed to the study, whether directly or indirectly, such as Annika Gomez, and especially to Heather McLane and Jose Vargas who made the lab during early mornings, late nights, and even the weekends an exciting place to be at. I also would like to thank Kevin Packard from the Cornell University Statistical Consulting Unit for his advices regarding the analysis of the data presented.

Works cited

Al Rwahnih, M., Dave, A., Anderson, M. M., Rowhani, A., Uyemoto, J. K., and Sudarshana, M. R. 2013. Association of a DNA virus with grapevines affected by red blotch disease in California. Phytopathology. 103:1069–1076.

Applied Biosystems. 2004. Guide to Performing Relative Quantitation of Gene Expression Using Real-Time Quantitative PCR.

Bustin, S. A., Benes, V., Garson, J. A., Hellemans, J., Huggett, J., Kubista, M., et al. 2009. The MIQE guidelines: minimum information for publication of quantitative real-time PCR experiments. Clin. Chem. 55:611–622.

Charles, J. G., Cohen, D., Walker, J. T. S., Forgie, S. A., Bell, V. A., and Breen, K. C. 2006. A review of Grapevine Leafroll associated Virus type 3 (GLRaV-3) for the New Zealand wine industry. Hortic. Food Res. Inst. N. Z. Ltd HortResearch. Client Report No. 18447.

Chooi, K. M., Cohen, D., and Pearson, M. N. 2016. Differential distribution and titre of selected grapevine leafroll-associated virus 3 genetic variants within grapevine rootstocks. Arch. Virol. :1-5

Constable, F. E., Connellan, J., Nicholas, P., and Rodoni, B. C. 2012. Comparison of enzyme-linked immunosorbent assays and reverse transcription-polymerase chain reaction for the reliable detection of Australian grapevine viruses in two climates during three growing seasons. Aust. J. Grape Wine Res. 18:239–244.

Constable, F. E., Connellan, J., Nicholas, P., and Rodoni, B. C. 2013. The reliability of woody indexing for detection of grapevine virus-associated diseases in three different climatic conditions in Australia. Aust. J. Grape Wine Res. 19:74–80.

Erdmann, J. B., Shepherd, D. N., Martin, D. P., Varsani, A., Rybicki, E. P., and Jeske, H. 2010. Replicative intermediates of maize streak virus found during leaf development. J. Gen. Virol. 91:1077–1081.

Feng, J.-L., Chen, S.-N., Tang, X.-S., Ding, X.-F., Du, Z.-Y., and Chen, J.-S. 2006. Quantitative Determination of Cucumber Mosaic Virus Genome RNAs in Virions by Real-Time Reverse Transcription-Polymerase Chain Reaction. Acta Biochim. Biophys. Sin. 38:669–676.

Gambino, G., Perrone, I., and Gribaudo, I. 2008. A Rapid and effective method for RNA extraction from different tissues of grapevine and other woody plants. Phytochem. Anal. PCA. 19:520–525.

Herrera-Vasquez, J. A., Rubio, L., Alfaro-Fernandez, A., Debreczeni, D. E., Font-San-Ambrosio, I., Falk, B. W., et al. 2015. Detection and absolute quantitation of Tomato torrado virus (ToTV) by real time. J. Virol. Methods. 221:90–94.

Hipper, C., Brault, V., Ziegler-Graff, V., and Revers, F. 2013. Viral and cellular factors involved in phloem transport of plant viruses. Front. Plant Sci. 4 Available at: http://www.frontiersin.org/plant_physiology/10.3389/fpls.2013.00154/abstract.

Hull, R. 2014. Chapter 13 - Assay, Detection, and Diagnosis of Plant Viruses. In *Plant Virology (Fifth Edition)*, ed. Roger Hull. Boston: Academic Press, p. 755–808. Available at: http://www.sciencedirect.com/science/article/pii/B9780123848710000133.

Krebelj, A. J., Čepin, U., Ravnikar, M., and Novak, M. P. 2015. Spatio-temporal distribution of Grapevine fanleaf virus (GFLV) in grapevine. Eur. J. Plant Pathol. 142:159–171.

Krenz, B., Thompson, J. R., Fuchs, M., and Perry, K. L. 2012. Complete Genome Sequence of a New Circular DNA Virus from Grapevine. J. Virol. 86:7715.

Krenz, B., Thompson, J. R., McLane, H. L., Fuchs, M., and Perry, K. L. 2014. Grapevine red blotch-associated virus Is Widespread in the United States. Phytopathology. 104:1232–1240.

Krupovic, M., Ravantti, J. J., and Bamford, D. H. 2009. Geminiviruses: a tale of a plasmid becoming a virus. BMC Evol. Biol. 9:1–11.

Lemoine, R., La Camera, S., Atanassova, R., Dedaldechamp, F., Allario, T., Pourtau, N., et al. 2013. Source-to-sink transport of sugar and regulation by environmental factors. Front. Plant Sci. 4:272.

Ling, K.-S., Zhu, H.-Y., Petrovic, N., and Gonsalves, D. 2001. Comparative Effectiveness of ELISA and RT-PCR for Detecting Grapevine Leafroll-Associated Closterovirus-3 in Field Samples. Am J Enol Vitic. 52:21–27.

Liu, D., Shi, L., Han, C., Yu, J., Li, D., and Zhang, Y. 2012. Validation of reference genes for gene expression studies in virus-infected Nicotiana benthamiana using quantitative real-time PCR. PloS One. 7:e46451.

Livak, K. J., and Schmittgen, T. D. 2001. Analysis of Relative Gene Expression Data Using Real-Time Quantitative PCR and the $2^{-\Delta\Delta CT}$ Method. Methods. 25:402–408.

Loescher, W. H., McCamant, T., and Keller, J. D. 1990. Carbohydrate Reserves, Translocation, and Storage in Woody Plant Roots. HortScience. 25:274–281.

Mackay, I. M., Arden, K. E., and Nitsche, A. 2002. Real-time PCR in virology. Nucleic Acids Res. 30:1292–1305.

Mansoor, S., Briddon, R. W., Zafar, Y., and Stanley, J. 2003. Geminivirus disease complexes: an emerging threat. Trends Plant Sci. 8:128–134.

Mansoor, S., Zafar, Y., and Briddon, R. W. 2006. Geminivirus disease complexes: the threat is spreading. Trends Plant Sci. 11:209–212.

Maree, H. J., Almeida, R. P. P., Bester, R., Chooi, K. M., Cohen, D., Dolja, V. V., et al. 2013. Grapevine leafroll-associated virus 3. Front. Microbiol. 4:82.

Mirmajlessi, S. M., Loit, E., Mänd, M., and Mansouripour, S. M. 2015. Real-time PCR applied to study on plant pathogens: potential applications in diagnosis - a review. Plant Prot. Sci. 51:177–190.

Monis, J., and Bestwick, R. K. 1996. Detection and localization of grapevine leafrollassociated closteroviruses in greenhouse and tissue culture grown plants. Am J Enol Vitic. 47:199–205.

Naidu, R., Rowhani, A., Fuchs, M., Golino, D., and Martelli, G. P. 2014. Grapevine Leafroll: A Complex Viral Disease Affecting a High-Value Fruit Crop. Plant Dis. 98:1172–1185.

Navarro, E., Serrano-Heras, G., Castaño, M. J., and Solera, J. 2015. Real-time PCR detection chemistry. Clin. Chim. Acta. 439:231–250.

Pabinger, S., Rödiger, S., Kriegner, A., Vierlinger, K., and Weinhäusel, A. 2014. A survey of tools for the analysis of quantitative PCR (qPCR) data. Biomol. Detect. Quantif. 1:23–33.

Pfaffl, M. W. 2001. A new mathematical model for relative quantification in real-time RT-PCR. Nucleic Acids Res. 29:e45.

Piepho, H. P., Büchse, A., and Emrich, K. 2003. A Hitchhiker's Guide to Mixed Models for Randomized Experiments. J. Agron. Crop Sci. 189:310–322.

Poojari, S., Alabi, O. J., Fofanov, V. Y., and Naidu, R. A. 2013. A Leafhopper-Transmissible DNA Virus with Novel Evolutionary Lineage in the Family Geminiviridae Implicated in Grapevine Redleaf Disease by Next-Generation Sequencing. PLoS ONE. 8:e64194.

Reid, K. E., Olsson, N., Schlosser, J., Peng, F., and Lund, S. T. 2006. An optimized grapevine RNA isolation procedure and statistical determination of reference genes for real-time RT-PCR during berry development. BMC Plant Biol. 6:27–27.

Rojas, M. R., Hagen, C., Lucas, W. J., and Gilbertson, R. L. 2005. Exploiting chinks in the plant's armor: evolution and emergence of geminiviruses. Annu Rev Phytopathol. 43 Available at: http://dx.doi.org/10.1146/annurev.phyto.43.040204.135939.

Rwahnih, M. A., Rowhani, A., Golino, D. A., Islas, C. M., Preece, J. E., and Sudarshana, M. R. 2015. Detection and genetic diversity of Grapevine red blotch-associated virus isolates in table grape accessions in the National Clonal Germplasm Repository in California. Can. J. Plant Pathol. 37:130–135.

Sambrook, J., and Russell, D. W. 2001. *Molecular Cloning: A Laboratory Manual*. Cold Spring Harbor Laboratory Press. Available at: https://books.google.com/books?id=Bosc5JVxNpkC.

Schmittgen, T. D., and Livak, K. J. 2008. Analyzing real-time PCR data by the comparative CT method. Nat Protoc. 3:1101–1108.

Searle, S. R., Casella, G., and McCulloch, C. E. 1992. *Variance Components*. Hoboken, New Jersey: John Wiley and Sons.

S. Savary and B. M. Cooke, eds. 2007. *Plant Disease Epidemiology: Facing Challenges of the 21st Century: Under the aegis of an International Plant Disease Epidemiology Workshop held at Landernau, France, 10-15th April, 2005*. 1st ed. Springer Netherlands.

Stanley, J., Bisaro, D. M., Briddon, R. W., Brown, J. K., Fauquet, C. M., Harrison, B. D., et al. 2005. In *Virus Taxonomy: VIIIth Report of the International Committee on Taxonomy of Viruses*, eds. C. M. Fauquet, M. A. Mayo, J. Maniloff, U. Desselberger, and L. A. Ball. London: Elsevier/Academic Press.

Sudarshana, M. R., Perry, K. L., and Fuchs, M. F. 2015. Grapevine Red Blotch-Associated Virus, an Emerging Threat to the Grapevine Industry. Phytopathology. 105:1026–1032.

Teliz, D., Tanne, E., Gonsalves, D., and Zee, F. 1987. Field serological detection of viral antigens associated with grapevine leafroll disease. Plant Dis. 71:704–709.

Tsai, C. W., Daugherty, M. P., and Almeida, R. P. P. 2012. Seasonal dynamics and virus translocation of Grapevine leafroll-associated virus 3 in grapevine cultivars. Plant Pathol. 61:977–985.

Yuan, J. S., Reed, A., Chen, F., and Stewart, N. C. 2006. Statistical analysis of real-time PCR data. BMC Bioinformatics. 7:1–12.